

Study of baryon acoustic oscillations with SDSS DR13 data and measurements of Ω_k and $\Omega_{\text{DE}}(a)$

B. Hoeneisen¹

¹ *Universidad San Francisco de Quito, Quito, Ecuador*
(Dated: December 13, 2016)

We measure the baryon acoustic oscillation (BAO) observables $\hat{d}_\alpha(z, z_c)$, $\hat{d}_z(z, z_c)$, and $\hat{d}_\parallel(z, z_c)$ as a function of redshift z in the range 0.1 to 0.7 with Sloan Digital Sky Survey (SDSS) data release DR13. These observables are independent and satisfy a consistency relation that provides discrimination against miss-fits due to background fluctuations. From these measurements and the correlation angle θ_{MC} of fluctuations of the Cosmic Microwave Background (CMB) we obtain $\Omega_k = -0.015 \pm 0.030$, $\Omega_{\text{DE}} + 2.2\Omega_k = 0.717 \pm 0.004$ and $w_1 = 0.37 \pm 0.61$ for dark energy density allowed to vary as $\Omega_{\text{DE}}(a) = \Omega_{\text{DE}}[1 + w_1(1 - a)]$. We present measurements of $\Omega_{\text{DE}}(a)$ at six values of the expansion parameter a . Fits with several scenarios and data sets are presented. The data is consistent with space curvature parameter $\Omega_k = 0$ and $\Omega_{\text{DE}}(a)$ constant.

INTRODUCTION

Peaks in the density of the primordial universe are the sources of acoustic waves of the tightly coupled plasma of photons, electrons, protons and helium nuclei. These acoustic waves propagate a distance $r'_S \approx 145$ Mpc until the time of recombination and decoupling t_{dec} [1, 2]. (All distances in this article are co-moving, i.e. are referred to the present time t_0 .) The baryon acoustic oscillation (BAO) distance r'_S corresponds to the observed correlation angle θ_{MC} of fluctuations of the cosmic microwave background (CMB) [2]. Dark matter follows the BAO waves. The results, well after decoupling, for an initial point-like peak in the density, are two concentric shells of overdensity of radius ≈ 145 Mpc and ≈ 18 Mpc [1, 3, 4]. The inner spherical shell becomes reprocessed by the hierarchical formation of galaxies [5], while the outer shell is unprocessed to better than 1% [4, 6] (or even 0.1% with corrections [4, 6]) and therefore is an excellent standard ruler to measure the expansion parameter $a(t)$ of the universe as a function of time t . Histograms of galaxy-galaxy distances show an excess in the approximate range $145 - 11$ Mpc to $145 + 11$ Mpc. We denote by d'_{BAO} the mean of this BAO signal. We set $r'_S = d'_{\text{BAO}} f$, where f is a correction factor due to the peculiar motions of galaxies (f depends on the orientation of the galaxy pair with respect to the line of sight). Measurements of these BAO signals are well established: see Refs. [3] and [4] for extensive lists of early publications.

In this article we present studies of BAO with Sloan Digital Sky Survey (SDSS) publicly released data DR13 [7]. The study has three parts:

(i) We measure the BAO observables $\hat{d}_\alpha(z, z_c)$, $\hat{d}_z(z, z_c)$, and $\hat{d}_\parallel(z, z_c)$ [8] in six bins of redshift z from 0.1 to 0.7. These observables are galaxy-galaxy correlation distances, in units of c/H_0 , of galaxy pairs respectively transverse to the line of sight, along the line of sight, and in an interval of angles with respect to the line of sight, for a reference (fictitious) cosmology.

(ii) We measure the space curvature parameter Ω_k and the dark energy density relative to the critical density $\Omega_{\text{DE}}(a)$ as a function of the expansion parameter a with the following BAO data used as an uncalibrated standard ruler: $\hat{d}_\alpha(z, z_c)$, $\hat{d}_z(z, z_c)$, and $\hat{d}_\parallel(z, z_c)$ for $0.1 < z < 0.7$ (this analysis), θ_{MC} for $z_{\text{dec}} = 1089.9 \pm 0.4$ from Planck satellite observations [2, 9], and measurements of BAO distances in the Lyman-alpha ($\text{Ly}\alpha$) forest with SDSS BOSS DR11 data at $z = 2.36$ [10] and $z = 2.34$ [11].

(iii) Finally we use the BAO measurements as a calibrated standard ruler to constrain a wider set of cosmological parameters.

The present analysis with DR13 data [7] closely follows the methods developed in Refs. [8] and [12] for data release DR12 [13].

BAO OBSERVABLES

To define the quantities being measured we write the (generalized) Friedmann equation that describes the expansion history of a homogeneous universe:

$$\frac{1}{H_0} \frac{1}{a} \frac{da}{dt} \equiv E(a) = \sqrt{\frac{\Omega_m}{a^3} + \frac{\Omega_r}{a^4} + \Omega_{\text{DE}}(a) + \frac{\Omega_k}{a^2}}. \quad (1)$$

The expansion parameter $a(t)$ is normalized so that $a(t_0) = 1$ at the present time t_0 . The Hubble parameter $H_0 \equiv 100h$ km s⁻¹ Mpc⁻¹ is normalized so that $E(1) = 1$ at the present time, i.e.

$$\Omega_m + \Omega_r + \Omega_{\text{DE}}(1) + \Omega_k = 1. \quad (2)$$

The terms under the square root in Eq. (1) are densities relative to the critical density of, respectively, non-relativistic matter, ultra-relativistic radiation, dark energy (whatever it is), and space curvature. In the General Theory of Relativity $\Omega_{\text{DE}}(a)$ is constant. Here we allow $\Omega_{\text{DE}}(a)$ be a function of a to be determined by observations. Measuring Ω_k and $\Omega_{\text{DE}}(a)$ is equivalent to measuring the expansion history of the universe $a(t)$.

The expansion parameter a is related to redshift z by $a = 1/(1+z)$.

The distance d' between two galaxies observed with a relative angle α and redshifts z_1 and z_2 can be written, with sufficient accuracy for our purposes, as [8]

$$\begin{aligned} d' &\equiv \frac{c}{H_0} d, \\ d &= \sqrt{d_\alpha^2 + d_z^2}, \\ d_\alpha &= 2 \sin\left(\frac{\alpha}{2}\right) \sqrt{\chi(z_1)\chi(z_2)} \left[1 + \frac{1}{6}\Omega_k \chi(z_1)\chi(z_2)\right], \\ d_z &= \chi(z_1) - \chi(z_2), \quad \text{where} \\ \chi(z) &\equiv \int_0^z \frac{dz'}{E(z')}. \end{aligned} \quad (3)$$

d_α and d_z are the distance components, in units of c/H_0 , transverse to the line of sight and along the line of sight, respectively. ($\chi(z)$ should not be confused with the χ^2 of fits.) The difference between the approximation (3) and the exact expression for d' , given by Eq. (3.19) of Ref. [14], is negligible for two galaxies at the distance d_{BAO} : the term of d_α proportional to Ω_k in Eq. (3) changes by 0.1% at $z = 0.7$.

We find the following approximations to $\chi(z)$ and $1/E(z)$ valid in the range $0 \leq z < 1$ with precision approximately $\pm 1\%$ for $z_c \approx 3.79$ [8]:

$$\chi(z) \approx z \exp\left(-\frac{z}{z_c}\right), \quad \frac{1}{E(z)} \approx \left(1 - \frac{z}{z_c}\right) \exp\left(-\frac{z}{z_c}\right). \quad (4)$$

Our strategy is as follows: We consider galaxies with redshift in a given range $z_{\min} < z < z_{\max}$. For each galaxy pair we calculate $d_\alpha(z, z_c)$, $d_z(z, z_c)$ and $d(z, z_c)$ with Eqs. (3) *with the approximation* (4) and fill one of three histograms of $d(z, z_c)$ (with weights to be discussed later) depending on the ratio $d_z(z, z_c)/d_\alpha(z, z_c)$:

- If $d_z(z, z_c)/d_\alpha(z, z_c) < 1/3$ fill a histogram of $d(z, z_c)$ that obtains a BAO signal centered at $\hat{d}_\alpha(z, z_c)$. For this histogram, $d_z^2(z, z_c)$ is a small correction relative to $d_\alpha^2(z, z_c)$ that is calculated with sufficient accuracy with the approximation (4), i.e. an error less than 0.2% on $\hat{d}_\alpha(z, z_c)$.
- If $d_\alpha(z, z_c)/d_z(z, z_c) < 1/3$ fill a second histogram of $d(z, z_c)$ that obtains a BAO signal centered at $\hat{d}_z(z, z_c)$. For this histogram, $d_\alpha^2(z, z_c)$ is a small correction relative to $d_z^2(z, z_c)$ that is calculated with sufficient accuracy with the approximation (4) and $\Omega_k = 0$, i.e. an error less than 0.2% on $\hat{d}_z(z, z_c)$.
- Else, fill a third histogram of $d(z, z_c)$ that obtains a BAO signal centered at $\hat{d}_/(z, z_c)$.

Note that these three histograms have different galaxy pairs, i.e. have independent signals and independent backgrounds.

The galaxy-galaxy correlation distance d_{BAO} , in units of c/H_0 , is obtained from the BAO observables $\hat{d}_\alpha(z, z_c)$, $\hat{d}_z(z, z_c)$, or $\hat{d}_/(z, z_c)$ as follows:

$$d_{\text{BAO}} = \hat{d}_\alpha(z, z_c) \frac{\chi(z) [1 + \frac{1}{6}\Omega_k \chi^2(z)]}{z \exp(-z/z_c)}, \quad (5)$$

$$d_{\text{BAO}} = \hat{d}_z(z, z_c) \frac{1}{(1 - z/z_c) \exp(-z/z_c) E(z)}, \quad (6)$$

$$\begin{aligned} d_{\text{BAO}} &= \hat{d}_/(z, z_c) \left(\frac{\chi(z) [1 + \frac{1}{6}\Omega_k \chi^2(z)]}{z \exp(-z/z_c)} \right)^{n/3} \\ &\times \left(\frac{1}{(1 - z/z_c) \exp(-z/z_c) E(z)} \right)^{1-n/3}. \end{aligned} \quad (7)$$

A numerical analysis obtains $n = 1.70$ for $z = 0.2$, dropping to $n = 1.66$ for $z = 0.8$ (in agreement with the method introduced in [1] that obtains $n \approx 2$ when d covers all angles). The redshifts z in Eqs. (5), (6) and (7) correspond to the weighted mean of z in the interval z_{\min} to z_{\max} . The fractions in Eqs. (5), (6) and (7) are within $\approx 1\%$ of 1 for $z_c = 3.79$. Note that the limits of $\hat{d}_\alpha(z, z_c)$ or $\hat{d}_z(z, z_c)$ or $\hat{d}_/(z, z_c)$ as $z \rightarrow 0$ are all equal to d_{BAO} .

The independent BAO observables $\hat{d}_\alpha(z, z_c)$, $\hat{d}_z(z, z_c)$, and $\hat{d}_/(z, z_c)$ satisfy the consistency relation

$$Q \equiv \frac{\hat{d}_/(z, z_c)}{\hat{d}_\alpha(z, z_c)^{n/3} \hat{d}_z(z, z_c)^{1-n/3}} = 1. \quad (8)$$

The approximations in Eqs. (4) obtain galaxy-galaxy correlation distances $\hat{d}_\alpha(z, z_c)$, $\hat{d}_z(z, z_c)$, and $\hat{d}_/(z, z_c)$ of a reference (fictitious) cosmology. We emphasize that these approximations are undone by Eqs. (5), (6), and (7) so in the end d_{BAO} has the correct dependence on the cosmological parameters which is different for Eqs. (5), (6), and (7).

The BAO observables $\hat{d}_\alpha(z, z_c)$, $\hat{d}_z(z, z_c)$, and $\hat{d}_/(z, z_c)$ were chosen because (i) they are dimensionless, (ii) they are independent, (iii) they do not depend on any cosmological parameter, (iv) they are almost independent of z (for an optimized value of $r_c \approx 3.79$) so that a large bin $z_{\max} - z_{\min}$ may be analyzed, and (v) satisfy the consistency relation (8) which allows discrimination against fits that converge on background fluctuations instead of the BAO signal.

It is observed that fluctuations in the CMB have a correlation angle [2, 9]

$$\theta_{\text{MC}} = 0.010410 \pm 0.000005, \quad (9)$$

(we have chosen a measurement by the Planck collaboration with no input from BAO). The extreme precision with which θ_{MC} is measured makes it one of the primary parameters of cosmology. The correlation distance r_S , in

units of c/H_0 , is obtained from θ_{MC} as follows:

$$r_S = 2 \sin\left(\frac{1}{2}\theta_{\text{MC}}\right) \chi(z_{\text{dec}}) \times \left[1 + \frac{1}{6}\Omega_k \chi^2(z_{\text{dec}}) + \frac{1}{120}\Omega_k^2 \chi^4(z_{\text{dec}})\right]. \quad (10)$$

For $\chi(z_{\text{dec}})$ we do not neglect $\Omega_r \equiv \Omega_\gamma N_{\text{eq}}/2$ of photons or neutrinos (we take $N_{\text{eq}} = 3.38$ [2] corresponding to 3 neutrino flavors).

GALAXY SELECTION AND DATA ANALYSIS

We obtain the following data from the SDSS DR13 catalog [7] for all objects identified as galaxies that pass quality selection flags: right ascension ra , declination dec , redshift z , redshift uncertainty $zErr$, and the absolute value of the magnitude r . We require a good measurement of redshift, i.e. $zErr < 0.001$. The present study is limited to galaxies with right ascension in the range 110° to 270° , declination in the range -5° to 70° , and redshift in the range 0.10 to 0.70. The galactic plane divides this data set into two independent sub-sets: the northern galactic cap (N) and the southern galactic cap (S) defined by $dec \geq 27.0^\circ - 17.0^\circ [(ra - 185.0^\circ)/(260.0^\circ - 185.0^\circ)]^2$.

We calculate the absolute luminosity F of galaxies relative to the absolute luminosity of a galaxy with $r = 19.0$ at $z = 0.35$, and calculate the corresponding magnitude r_{35} . We consider galaxies with $17.0 < r_{35} < 23.0$ (G). We define “luminous galaxies” (LG) with, for example, $r_{35} < 19.2$, and “clusters” (C). Clusters C are based on a cluster finding algorithm that starts with LG’s as seeds, calculates the total absolute luminosity of all G’s within a distance 0.006 (in units of c/H_0), and then selects local maximums of these total absolute luminosities above a threshold, e.g. $r_{35} < 16.6$.

A “run” is defined by a range of redshifts ($z_{\text{min}}, z_{\text{max}}$), a data set, and a definition of galaxy and “center”. For each of 6 bins of redshift z from 0.10 to 0.70, and each of 5 offset bins of z from 0.15 to 0.65, and for each data set N or S, and for each choice of galaxy-center G-G, G-LG, LG-LG, or G-C (with several absolute luminosity cuts), we fill histograms of galaxy-center distances $d(z, z_c)$ and obtain the BAO distances $\hat{d}_\alpha(z, z_c)$, $\hat{d}_z(z, z_c)$, and $\hat{d}_\gamma(z, z_c)$ by fitting these histograms.

Histograms are filled with weights $(0.033/d)^2$ or $F_i F_j (0.033/d)^2$, where F_i and F_j are the absolute luminosities F of galaxy i and center j respectively. We obtain histograms with $z_c = 3.79, 3.0$ and 5.0 . The reason for this large degree of redundancy is the difficulty to discriminate the BAO signal from the background with its statistical and cosmological fluctuations due to galaxy clustering. Pattern recognition is aided by multiple histograms with different background fluctuations, and by the characteristic shape of the BAO signal that has a

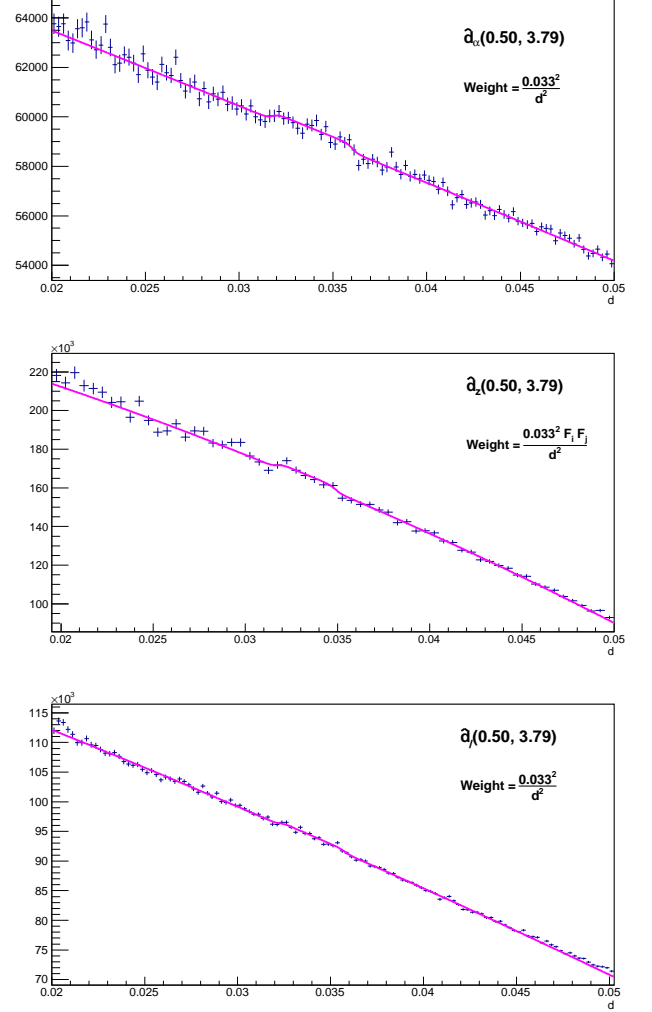


FIG. 1: Fits to histograms of $d(0.5, 3.79)$ that obtain $\hat{d}_\alpha(0.5, 3.79)$, $\hat{d}_z(0.5, 3.79)$, and $\hat{d}_\gamma(0.5, 3.79)$ in the northern galactic cap.

lower edge at approximately 0.031 and an upper edge at approximately 0.036 as shown in Fig. 1.

The fitting function is a second degree polynomial for the background and, for the BAO signal, a step-up-step-down function of the form

$$\frac{\exp(x_<)}{\exp(x_<) + \exp(-x_<)} - \frac{\exp(x_>)}{\exp(x_>) + \exp(-x_>)}$$

where

$$x_< = \frac{d - \hat{d} + \Delta d}{\sigma}, \quad x_> = \frac{d - \hat{d} - \Delta d}{\sigma}.$$

A run is defined as “successful” if the fits to *all three histograms* converge with a signal-to-background ratio significance greater than 1 standard deviation (raising this cut further obtains little improvement due to the cos-

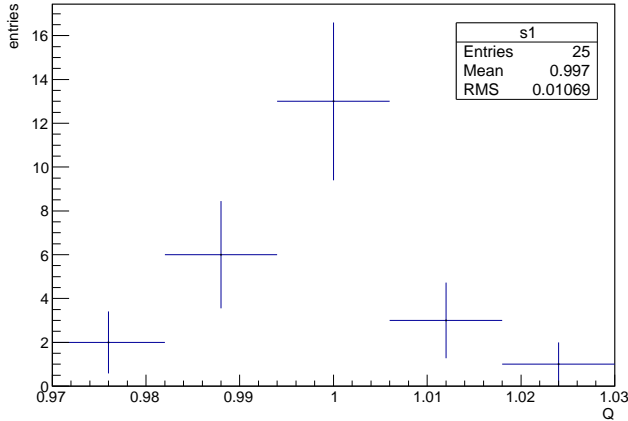


FIG. 2: Distribution of the consistency parameter Q for the 25 N or S successful runs.

mological fluctuations of the background), and the consistency parameter Q is in the range 0.97 to 1.03 (if Q is outside of this range then at least one of the fits has converged on a fluctuation of the background instead of the BAO signal). We obtain 13 successful runs for N and 12 successful runs for S which are presented in Tables I and II respectively. The histogram of the consistency parameter Q for these 25 runs is presented in Fig. 2.

For each bin of redshift z we select from Tables I or II the run with least $|Q - 1|$ and obtain the 18 independent BAO distances listed in Table III. This Table III is the main result of the present analysis, and superceeds the corresponding tables for DR12 in Refs. [8] and [12].

UNCERTAINTIES

Histograms of BAO distances $d(z, z_c)$ have statistical fluctuations, and fluctuations of the background due to the clustering of galaxies as seen in Fig. 1. These two types of fluctuations are the dominant source of the total uncertainties of the BAO distance measurements. These uncertainties are independent for each entry in Table III. We present several estimates of the total uncertainties of the entries in Tables I, II, and III extracted directly from the fluctuations of the numbers in these tables. All uncertainties in this article are at 68% confidence level.

We neglect the variation of $\hat{d}_\alpha(z, z_c)$, $\hat{d}_z(z, z_c)$, and $\hat{d}_l(z, z_c)$ between adjacent bins of z with respect to their uncertainties. The root-mean-square (r.m.s.) differences divided by $\sqrt{2}$ between corresponding rows in Tables I and II for $\hat{d}_\alpha(z, z_c)$, $\hat{d}_z(z, z_c)$, and $\hat{d}_l(z, z_c)$ are 0.00055, 0.00093, and 0.00054 respectively. We assign these numbers as total uncertainties of each entry in Tables I and II.

The 18 entries in Table III are independent. The r.m.s. differences for rows 1-2, 3-4 and 5-6 divided by $\sqrt{2}$ are 0.00030, 0.00052, and 0.00020 for $\hat{d}_\alpha(z, z_c)$, $\hat{d}_z(z, z_c)$, and $\hat{d}_l(z, z_c)$ respectively.

The average and standard deviation of the columns $\hat{d}_\alpha(z, z_c)$, $\hat{d}_z(z, z_c)$, and $\hat{d}_l(z, z_c)$ in Table III are respectively 0.03342, 0.00021; 0.03355, 0.00051; and 0.03348, 0.00023.

The r.m.s. of $(1 - Q)$ for Tables N and S is 0.0111. The average of all entries in Tables N and S is 0.03383. From the above estimates we take the uncertainties of $\hat{d}_\alpha(z, z_c)$, $\hat{d}_z(z, z_c)$, and $\hat{d}_l(z, z_c)$ to be in the ratio 1 : 2 : 1. From these numbers we calculate the independent total uncertainties of $\hat{d}_\alpha(z, z_c)$, $\hat{d}_z(z, z_c)$, and $\hat{d}_l(z, z_c)$ to be 0.00026, 0.00052, and 0.00026 respectively.

From these estimates, we take the following independent total uncertainties for each entry of $\hat{d}_\alpha(z, z_c)$, $\hat{d}_z(z, z_c)$, and $\hat{d}_l(z, z_c)$ in Table III: 0.00030, 0.00060, and 0.00030 respectively.

CORRECTIONS

Let us consider corrections to the BAO distances due to peculiar velocities and peculiar displacements of galaxies towards their centers. A relative peculiar velocity v_p towards the center causes a reduction of the BAO distances $\hat{d}_\alpha(z, z_c)$, $\hat{d}_z(z, z_c)$, and $\hat{d}_l(z, z_c)$ of order $0.5v_p/c$. In addition, the Doppler shift produces an apparent shortening of $\hat{d}_z(z, z_c)$ by v_p/c , and somewhat less for $\hat{d}_l(z, z_c)$.

We multiply the measured BAO distances $\hat{d}_\alpha(z, z_c)$, $\hat{d}_z(z, z_c)$, and $\hat{d}_l(z, z_c)$ by correction factors f_α , f_z and f_l respectively. Simulations in Ref. [6] obtain $f_\alpha - 1 = 0.2283 \pm 0.0609\%$ and $f_z - 1 = 0.2661 \pm 0.0820\%$ at $z = 0.3$, $f_\alpha - 1 = 0.1286 \pm 0.0425\%$ and $f_z - 1 = 0.1585 \pm 0.0611\%$ at $z = 1$, and $f_\alpha - 1 = 0.0435 \pm 0.0293\%$ and $f_z - 1 = 0.0582 \pm 0.0402\%$ at $z = 3$. In the following sections we present fits with the corrections

$$\begin{aligned} f_\alpha - 1 &= 0.00320 \cdot a^{1.35}, \\ f_z - 1 &= 0.00381 \cdot a^{1.35}, \\ f_l - 1 &= 0.00350 \cdot a^{1.35}. \end{aligned} \quad (11)$$

The effect of these corrections can be seen by comparing the first two fits in Table IV below. An order-of-magnitude estimate of this correction can be obtained by calculating the r.m.s. v_p corresponding to modes with $k \equiv 2\pi/\lambda < 2\pi/(4d'_{\text{BAO}})$ with Eq. (11) of Ref. [5] and normalizing the result to σ_8 , i.e. to the r.m.s. density fluctuation in a volume $(8\text{Mpc}/h)^3$.

MEASUREMENTS OF Ω_k AND $\Omega_{\text{DE}(a)}$ FROM UNCALIBRATED BAO

We consider five scenarios:

TABLE I: Measured BAO distances $\hat{d}_\alpha(z, z_c)$, $\hat{d}_z(z, z_c)$, and $\hat{d}_/(z, z_c)$ in units of c/H_0 with $z_c = 3.79$ (see text) from SDSS DR13 galaxies with right ascension 110^0 to 270^0 , and declination -5^0 to 70^0 in the northern galactic cap, i.e. $\text{dec} > 27.0^0 - 17.0^0 [(ra - 185.0^0)/(260.0^0 - 185.0^0)]^2$. Uncertainties are statistical from the fits to the BAO signal. Each BAO distance has an independent total uncertainty 0.00055 for $\hat{d}_\alpha(z, z_c)$ and $\hat{d}_/(z, z_c)$, or 0.00093 for $\hat{d}_z(z, z_c)$. No corrections have been applied.

z	z_{\min}	z_{\max}	galaxies	centers	type	$100\hat{d}_\alpha(z, z_c)$	$100\hat{d}_z(z, z_c)$	$100\hat{d}_/(z, z_c)$	Q
0.14	0.10	0.20	152785	3729	G-C	3.367 ± 0.014	3.284 ± 0.014	3.306 ± 0.018	0.993
0.14	0.10	0.20	152785	2853	G-C	3.376 ± 0.017	3.375 ± 0.010	3.363 ± 0.017	0.996
0.25	0.20	0.30	58670	3271	G-C	3.271 ± 0.019	3.499 ± 0.020	3.414 ± 0.020	1.014
0.31	0.25	0.35	69271	3677	G-C	3.344 ± 0.025	3.521 ± 0.017	3.409 ± 0.016	0.997
0.35	0.30	0.40	83515	58491	G-LG	3.354 ± 0.013	3.320 ± 0.010	3.350 ± 0.012	1.003
0.40	0.35	0.45	91672	4180	G-C	3.479 ± 0.025	3.358 ± 0.028	3.380 ± 0.025	0.987
0.46	0.40	0.50	137972	137972	G-G	3.523 ± 0.011	3.420 ± 0.019	3.485 ± 0.007	1.002
0.46	0.40	0.50	137972	55925	G-LG	3.450 ± 0.014	3.423 ± 0.011	3.456 ± 0.007	1.005
0.50	0.45	0.55	195144	1514	G-C	3.436 ± 0.024	3.285 ± 0.015	3.431 ± 0.012	1.018
0.50	0.45	0.55	195144	5935	G-C	3.391 ± 0.019	3.332 ± 0.020	3.401 ± 0.014	1.011
0.55	0.50	0.60	188410	1105	G-C	3.338 ± 0.021	3.293 ± 0.018	3.300 ± 0.026	0.971
0.64	0.60	0.70	81624	81624	G-G	3.368 ± 0.014	3.572 ± 0.021	3.439 ± 0.012	0.995
0.64	0.60	0.70	81624	33982	G-LG	3.378 ± 0.009	3.586 ± 0.016	3.481 ± 0.009	1.004

TABLE II: Measured BAO distances $\hat{d}_\alpha(z, z_c)$, $\hat{d}_z(z, z_c)$, and $\hat{d}_/(z, z_c)$ in units of c/H_0 with $z_c = 3.79$ (see text) from SDSS DR13 galaxies with right ascension 110^0 to 270^0 , and declination -5^0 to 70^0 in the southern galactic cap, i.e. $\text{dec} < 27.0^0 - 17.0^0 [(ra - 185.0^0)/(260.0^0 - 185.0^0)]^2$. Uncertainties are statistical from the fits to the BAO signal. Each BAO distance has an independent total uncertainty 0.00055 for $\hat{d}_\alpha(z, z_c)$ and $\hat{d}_/(z, z_c)$, or 0.00093 for $\hat{d}_z(z, z_c)$. No corrections have been applied.

z	z_{\min}	z_{\max}	galaxies	centers	type	$100\hat{d}_\alpha(z, z_c)$	$100\hat{d}_z(z, z_c)$	$100\hat{d}_/(z, z_c)$	Q
0.19	0.15	0.25	58381	1538	G-C	3.338 ± 0.024	3.315 ± 0.037	3.321 ± 0.011	0.998
0.25	0.20	0.30	38931	3865	G-C	3.311 ± 0.035	3.381 ± 0.016	3.360 ± 0.013	1.006
0.31	0.25	0.35	46916	2828	G-C	3.277 ± 0.017	3.438 ± 0.027	3.333 ± 0.018	0.996
0.31	0.25	0.35	46916	2559	G-C	3.271 ± 0.028	3.309 ± 0.042	3.295 ± 0.036	1.002
0.46	0.40	0.50	91599	91599	G-G	3.319 ± 0.013	3.509 ± 0.022	3.366 ± 0.016	0.990
0.46	0.40	0.50	91599	37456	G-LG	3.323 ± 0.019	3.445 ± 0.024	3.369 ± 0.016	0.998
0.46	0.40	0.50	37456	37456	LG-LG	3.390 ± 0.019	3.536 ± 0.013	3.367 ± 0.014	0.975
0.64	0.60	0.70	53518	53518	G-G	3.424 ± 0.015	3.327 ± 0.019	3.373 ± 0.016	0.997
0.64	0.60	0.70	53518	23384	G-LG	3.393 ± 0.017	3.427 ± 0.028	3.373 ± 0.019	0.990
0.64	0.60	0.70	53518	941	G-C	3.349 ± 0.014	3.316 ± 0.046	3.346 ± 0.020	1.003
0.64	0.60	0.70	23384	23384	LG-LG	3.446 ± 0.016	3.371 ± 0.026	3.381 ± 0.015	0.991
0.64	0.60	0.70	53518	689	G-C	3.416 ± 0.020	3.317 ± 0.021	3.316 ± 0.036	0.983

TABLE III: Independent measured BAO distances $\hat{d}_\alpha(z, z_c)$, $\hat{d}_z(z, z_c)$, and $\hat{d}_/(z, z_c)$ in units of c/H_0 with $z_c = 3.79$ (see text) obtained by selecting, for each bin of z , the entry with least $|Q - 1|$ in Tables I or II. Each BAO distance has an independent total uncertainty 0.00030 for $\hat{d}_\alpha(z, z_c)$ and $\hat{d}_/(z, z_c)$, or 0.00060 for $\hat{d}_z(z, z_c)$. No corrections have been applied.

z	z_{\min}	z_{\max}	$100\hat{d}_\alpha(z, z_c)$	$100\hat{d}_z(z, z_c)$	$100\hat{d}_/(z, z_c)$
0.14	0.1	0.2	3.376	3.375	3.363
0.25	0.2	0.3	3.311	3.381	3.360
0.35	0.3	0.4	3.354	3.320	3.350
0.46	0.4	0.5	3.323	3.445	3.369
0.55	0.5	0.6	3.338	3.293	3.300
0.64	0.6	0.7	3.349	3.316	3.346

1. The observed acceleration of the expansion of the universe is due to the cosmological constant, i.e.

$\Omega_{\text{DA}}(a)$ is constant.

2. The observed acceleration of the expansion of the universe is due to a gas of negative pressure with an equation of state $w \equiv p/\rho < 0$. We allow the index w be a function of a [3, 15, 16]: $w(a) = w_0 + w_a(1 - a)$. While this gas dominates $E(a)$ the equation [2]

$$\frac{d\rho}{dt} = -3\frac{da/dt}{a}(\rho + p) \quad (12)$$

can be integrated with the result [3, 15, 16]

$$\Omega_{\text{DE}}(a) = \Omega_{\text{DE}} a^{-3(1+w_0+w_a)} \exp\{-3w_a(1-a)\}. \quad (13)$$

If $w_0 = -1$ and $w_a = 0$ we obtain constant $\Omega_{\text{DA}}(a)$ as in the General Theory of Relativity.

3. Same as Scenario 2 with $w(a)$ constant, i.e. $w_a = 0$.

TABLE IV: Cosmological parameters obtained from the 18 independent BAO measurements in Table III in several scenarios. Corrections for peculiar motions are given by Eq. (11) except, for comparison, the fit “1*” which has no correction. Scenario 1 has $\Omega_{\text{DE}}(a)$ constant. Scenario 3 has $w = w_0$. Scenario 4 has $\Omega_{\text{DE}}(a) = \Omega_{\text{DE}}[1 + w_1(1 - a)]$.

	Scenario 1*	Scenario 1	Scenario 1	Scenario 3	Scenario 4	Scenario 4
Ω_k	0 fixed	0 fixed	0.173 ± 0.173	0 fixed	0 fixed	0.151 ± 0.185
$\Omega_{\text{DE}} + 0.5\Omega_k$	0.714 ± 0.014	0.716 ± 0.014	0.710 ± 0.016	0.772 ± 0.094	0.749 ± 0.049	0.732 ± 0.052
w_0	n.a.	n.a.	n.a.	-0.84 ± 0.22	n.a.	n.a.
w_1	n.a.	n.a.	n.a.	n.a.	0.44 ± 0.60	0.33 ± 0.70
$100d_{\text{BAO}}$	3.38 ± 0.02	3.39 ± 0.02	3.38 ± 0.03	3.36 ± 0.05	3.36 ± 0.05	3.36 ± 0.05
$\chi^2/\text{d.f.}$	10.9/16	11.2/16	10.2/15	10.6/15	10.7/15	10.0/14

TABLE V: Cosmological parameters obtained from the 18 BAO measurements in Table III plus θ_{MC} from Eq. (9) in several scenarios. Corrections for peculiar motions are given by Eq. (11). Scenario 1 has $\Omega_{\text{DE}}(a)$ constant. Scenario 2 has $w(a) = w_0 + w_a(1 - a)$. Scenario 3 has $w = w_0$. Scenario 4 has $\Omega_{\text{DE}}(a) = \Omega_{\text{DE}}[1 + w_1(1 - a)]$.

	Scenario 1	Scenario 1	Scenario 2	Scenario 3	Scenario 4	Scenario 4
Ω_k	0 fixed	0.002 ± 0.007	0 fixed	0 fixed	0 fixed	-0.015 ± 0.030
$\Omega_{\text{DE}} + 2.2\Omega_k$	0.719 ± 0.003	0.718 ± 0.004	0.708 ± 0.015	0.718 ± 0.004	0.718 ± 0.004	0.717 ± 0.004
w_0	n.a.	n.a.	-0.87 ± 0.19	-0.99 ± 0.04	n.a.	n.a.
w_a or w_1	n.a.	n.a.	-0.60 ± 0.93	n.a.	0.06 ± 0.15	0.37 ± 0.61
$100d_{\text{BAO}}$	3.40 ± 0.02	3.39 ± 0.02	3.36 ± 0.06	3.39 ± 0.03	3.39 ± 0.03	3.37 ± 0.05
$\chi^2/\text{d.f.}$	11.2/17	11.2/16	10.7/15	11.1/16	11.1/16	10.8/15

4. We assume $\Omega_{\text{DA}}(a) = \Omega_{\text{DA}}[1 + w_1(1 - a)]$.

5. $\Omega_{\text{DA}}(a)$ is arbitrary and needs to be measured at every a .

Note that BAO measurements can constrain $\Omega_{\text{DE}}(a)$ for $0.3 \lesssim a \leq 1$ where $\Omega_{\text{DE}}(a)$ contributes significantly to $E(a)$.

Let us try to understand qualitatively how the BAO distance measurements presented in Table III constrain the cosmological parameters. In the limit $z \rightarrow 0$ we obtain $d_{\text{BAO}} = \hat{d}_\alpha(0, z_c) = \hat{d}_z(0, z_c) = \hat{d}_\gamma(0, z_c)$, so the first row with $z = 0.14$ in Table III approximately determines d_{BAO} . This d_{BAO} and the measurement of, for example, $\hat{d}_z(0.3, z_c)$ then constrains the derivative of $\Omega_{\text{m}}/a^3 + \Omega_{\text{DE}} + \Omega_k/a^2$ with respect to a at $z \approx 0.3$, i.e. constrains approximately $\Omega_{\text{DE}} + 0.5\Omega_k$. We need an additional constraint for Scenario 1. d_{BAO} and θ_{MC} constrain the last two factors in Eq. (10), i.e. approximately constrain $\Omega_{\text{DE}} + 2.1\Omega_k$. The additional BAO distance measurements in Table III then also constrain w_0 and w_a , or w_1 .

In Table IV we present the cosmological parameters obtained by minimizing the χ^2 with 18 terms corresponding to the 18 independent BAO distance measurements in Table III for several scenarios. We find that the data is in agreement with the simplest cosmology with $\Omega_k = 0$ and $\Omega_{\text{DE}}(a)$ constant with χ^2 per degree of freedom (d.f.) 11.2/16, so no additional parameter is needed to obtain a good fit to this data. For free Ω_k we obtain $\Omega_{\text{DE}} + 0.5\Omega_k = 0.710 \pm 0.016$ for constant $\Omega_{\text{DE}}(a)$, or 0.732 ± 0.052 if $\Omega_{\text{DE}}(a)$ is allowed to depend on a as in

Scenario 4. We present the variable $\Omega_{\text{DE}} + 0.5\Omega_k$ instead of Ω_{DE} because it has a smaller uncertainty. The constraints on Ω_k are weak.

In Table V we present the cosmological parameters obtained by minimizing the χ^2 with 19 terms corresponding to the 18 BAO distance measurements listed in Table III plus the measurement of the correlation angle θ_{MC} of the CMB given in Eq. (9). We present the variable $\Omega_{\text{DE}} + 2.2\Omega_k$ instead of Ω_{DE} because it has a smaller uncertainty. We obtain

$$\begin{aligned}\Omega_k &= -0.015 \pm 0.030, \\ \Omega_{\text{DE}} + 2.2\Omega_k &= 0.717 \pm 0.004, \\ w_1 &= 0.37 \pm 0.61,\end{aligned}\tag{14}$$

when $\Omega_{\text{DE}}(a)$ is allowed to vary as in Scenario 4. There is no tension between the data and the case $\Omega_k = 0$ and constant $\Omega_{\text{DE}}(a)$: with these two constraints we obtain $\Omega_{\text{DE}} = 0.719 \pm 0.003$ with $\chi^2/\text{d.f.} = 11.2/17$.

We now add BAO measurements with SDSS BOSS DR11 data of quasar Ly α forest cross-correlation at $z = 2.36$ [10] and Ly α forest autocorrelation at $z = 2.34$ [11]. From the combination in Fig. 13 of Ref. [11] we obtain

$$\begin{aligned}\frac{\chi(2.34)(1 + \Omega_k\chi^2(2.34)/6)}{d_{\text{BAO}}(1 + 2.34)} &= 10.95 \pm 0.36, \\ \frac{1}{E(z = 2.34)d_{\text{BAO}}} &= 9.14 \pm 0.20.\end{aligned}\tag{15}$$

From the 18 BAO plus θ_{MC} plus 2 Ly α measurements, for free Ω_k , and $\Omega_{\text{DE}}(a)$ allowed to vary as in Scenario 4,

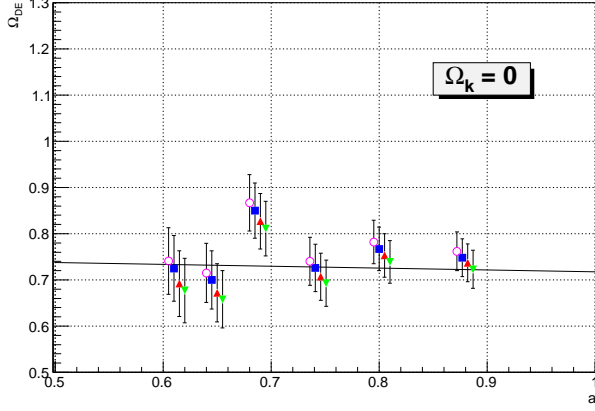


FIG. 3: Measurements of $\Omega_{\text{DE}}(a)$ obtained from the 6 $\hat{d}_z(z, z_c)$ in Table III for $\Omega_k = 0$, and the corresponding d_{BAO} and Ω_{DE} from the fit for Scenario 4 in Table V. The straight line is $\Omega_{\text{DE}}(a) = 0.718[1 + 0.055(1 - a)]$ from the central values of this fit. The uncertainties correspond only to the total uncertainties of $\hat{d}_z(z, z_c)$. To illustrate correlated uncertainties we present results for $(d_{\text{BAO}}, \Omega_{\text{DE}}) = (0.0339, 0.718 \pm 0.004)$ (squares), $(0.0339, 0.718 - 0.004)$ (triangles), $(0.0339 + 0.0003, 0.718)$ (inverted triangles), and $(0.0339 - 0.0003, 0.718)$ (circles). For clarity some offsets in a have been applied.

we obtain $\Omega_k = -0.013 \pm 0.009$, $\Omega_{\text{DE}} + 2.2\Omega_k = 0.717 \pm 0.004$, and $w_1 = 0.34 \pm 0.24$. The $\chi^2/\text{d.f.}$ is 17.6/17. Note that the Ly α measurements reduce the uncertainties of Ω_k and w_1 . Requiring $\Omega_k = 0$ and $\Omega_{\text{DE}}(a)$ constant raises the $\chi^2/\text{d.f.}$ to 19.7/19, so we observe no tension between the data and these two requirements, and obtain $\Omega_{\text{DE}} + 2.2\Omega_k = 0.719 \pm 0.003$.

DETAILED MEASUREMENT OF $\Omega_{\text{DE}}(a)$

We obtain $\Omega_{\text{DE}}(a)$ from the 6 independent measurements of $\hat{d}_z(z, z_c)$ in Table III, and Eqs. (6) and (1) for the case $\Omega_k = 0$. The values of d_{BAO} and $\Omega_{\text{m}} = 1 - \Omega_{\text{DE}}(1) - \Omega_k$ are obtained from the fit for Scenario 4 in Table V. The results are presented in Fig. 3. To guide the eye, we also show the straight line corresponding to the central values of Ω_{DE} and w_1 of the fit for Scenario 4. In Fig. 4 we present the results for offset bins of z (which are partially correlated with the entries in Fig. 3).

MEASUREMENTS OF Ω_k , $\Omega_{\text{DE}}(a)$ AND N_{eq} FROM CALIBRATED BAO

Up to this point we have used the BAO distance $d_{\text{BAO}}f = r_s$ as an uncalibrated standard ruler. The

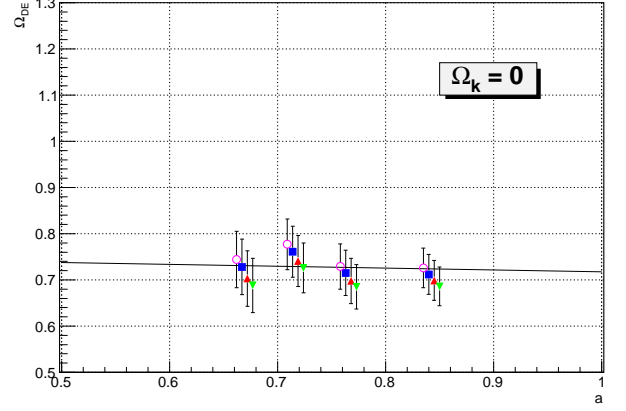


FIG. 4: Same as Fig. 3 for offset bins of z with least $|Q - 1|$ in Tables I or II. These measurements are partially correlated with those of Fig. 3.

cosmological parameters h and $\Omega_{\text{b}}h^2$ drop out of such an analysis, and the dependences of the results on N_{eq} are not significant. $\Omega_{\text{b}} \equiv \rho_{\text{b0}}/\rho_{\text{crit}}$ is the present density of baryons relative to the critical density. In this section we consider the BAO distance as a calibrated standard ruler to constrain the cosmological parameters Ω_k , $\Omega_{\text{DE}}(a)$, N_{eq} , h and $\Omega_{\text{b}}h^2$.

The sound horizon is calculated from first principles [1] as follows:

$$r'_S = \int_0^{t_{\text{dec}}} \frac{c_s dt}{a} = \int_0^{a_{\text{dec}}} \frac{c_s da}{H_0 a^2 E(a)}, \quad (16)$$

where the speed of sound is

$$c_s = \frac{c}{\sqrt{3(1 + 3\rho_{\text{b0}}a/(4\rho_{\gamma 0}))}}. \quad (17)$$

We can write the result for our purposes as

$$r_S = 0.03389 \times A \times \left(\frac{0.30}{\Omega_{\text{m}}}\right)^{0.255} \quad (18)$$

where

$$A = \left(\frac{h}{0.72}\right)^{0.489} \left(\frac{0.023}{\Omega_{\text{b}}h^2}\right)^{0.098} \left(\frac{3.36}{N_{\text{eq}}}\right)^{0.245} \quad (19)$$

(we have neglected the dependence of $z_{\text{dec}} = 1089.9 \pm 0.4$ [2, 9] on the cosmological parameters).

In this paragraph we take $N_{\text{eq}} = 3.38$ corresponding to 3 flavors of neutrinos [2]. From Big-Bang nucleosynthesis, $\Omega_{\text{b}}h^2 = 0.0225 \pm 0.0008$ (at 68% confidence) [2]. With the latest direct measurement $h = 0.720 \pm 0.030$ by the Hubble Space Telescope Key Project [17] we obtain $A = 1.000 \pm 0.021$. An alternative choice is the Planck “TT+lowP+lensing” analysis [2], that assumes $\Omega_k = 0$ and a Λ CDM cosmology, that obtains

$\Omega_b h^2 = 0.02226 \pm 0.00023$, $h = 0.678 \pm 0.009$ and $A = 0.973 \pm 0.007$. The cosmological parameters that minimize the χ^2 with 22 terms (18 BAO measurements from Table III plus θ_{MC} from Eq. (9) plus 2 $\text{Ly}\alpha$ measurements from Eq. (15) plus A) are presented in Table VI. Note that the addition of the external constraint from A slightly reduces the uncertainties of Ω_k and w_1 if $N_{eq} = 3.38$ is fixed. Note in Table VI that the data is consistent with the constraints $\Omega_k = 0$ and constant $\Omega_{DE}(a)$ for both values of A .

In this paragraph we let N_{eq} be free. We turn the problem around: from 18 BAO measurements from Table III plus θ_{MC} from Eq. (9) plus 2 $\text{Ly}\alpha$ measurements from Eq. (15) we constrain A . The results are $A = 0.965 \pm 0.014$ for free Ω_k and $\Omega_{DE}(a)$ allowed to vary as in Scenario 4, $A = 0.983 \pm 0.005$ for $\Omega_k = 0$ fixed and $\Omega_{DE}(a)$ allowed to vary as in Scenario 4, and $A = 0.9855 \pm 0.0012$ for $\Omega_k = 0$ fixed and constant $\Omega_{DE}(a)$. For free Ω_k , $\Omega_{DE}(a)$ allowed to vary as in Scenario 4, $\Omega_b h^2 = 0.0225 \pm 0.0008$, and $h = 0.720 \pm 0.030$ we obtain $N_{eq} = 3.92 \pm 0.40$ corresponding to $N_{eff} = 4.2 \pm 0.9$ neutrino flavors. For $\Omega_k = 0$ fixed, constant $\Omega_{DE}(a)$, $\Omega_b h^2 = 0.02226 \pm 0.00023$, and $h = 0.678 \pm 0.009$ we obtain $N_{eq} = 3.20 \pm 0.09$ corresponding to $N_{eff} = 2.64 \pm 0.20$ neutrino flavors.

COMPARISON WITH PREVIOUS MEASUREMENTS

Let us compare the results obtained with SDSS DR13 data with DR12 data. The χ^2 between Table III and Table III of Ref. [8] is 44.8 for 18 degrees of freedom. The χ^2 between Table III and Table III of Ref. [12] is 25.9 for 17 degrees of freedom. The disagreement in both cases is due to the same two entries in Tables III of Ref. [8] or III of Ref. [12] with miss-fits converging on background fluctuations instead of the BAO signal: $\hat{d}_\alpha(0.46, 3.79)$ and $\hat{d}_\gamma(0.55, 3.79)$. The fluctuation of $\hat{d}_\alpha(0.46, 3.79)$ can be seen in Table I for the northern galactic cap, but not in Table II for the southern galactic cap. Removing the two miss-fits from the comparisons obtains $\chi^2/\text{d.f.} = 21.2/16$ and $11.1/15$ respectively.

We compare Eq. (14) for DR13 data, with the corresponding fits for DR12 data. From Table VIII of Ref. [8]:

$$\begin{aligned}\Omega_k &= 0.043 \pm 0.041, \\ \Omega_{DE} + 2.0\Omega_k &= 0.716 \pm 0.006, \\ w_1 &= -0.16 \pm 0.94.\end{aligned}\quad (20)$$

From Table VII of Ref. [12]:

$$\begin{aligned}\Omega_k &= 0.060 \pm 0.052, \\ \Omega_{DE} + 2.0\Omega_k &= 0.717 \pm 0.007, \\ w_1 &= -0.86 \pm 1.26.\end{aligned}\quad (21)$$

Note in Eq. (14) how the DR13 data has lowered the uncertainties.

The final consensus measurements of SDSS DR12 data [18] are presented in Table VII (reproduced from Ref. [12] for completeness). There is agreement with the measurements of DR13 data in Table III. The notation of Ref. [18] is related to the notation of the present article as follows:

$$\begin{aligned}D_M \frac{r_{d,\text{fid}}}{r_d} &= \frac{c}{H_0} \chi(z) \left[1 + \frac{1}{6} \Omega_k \chi^2(z) \right] \frac{r_{d,\text{fid}}}{d'_{\text{BAO}}} \\ &= r_{d,\text{fid}} \frac{z \exp(-z/z_c)}{\hat{d}_\alpha(z, z_c)},\end{aligned}\quad (22)$$

$$\begin{aligned}H \frac{r_d}{r_{d,\text{fid}}} &= H_0 E(z) \frac{d'_{\text{BAO}}}{r_{d,\text{fid}}} \\ &= \frac{c}{r_{d,\text{fid}}} \frac{\hat{d}_z(z, z_c)}{(1 - z/z_c) \exp(-z/z_c)},\end{aligned}\quad (23)$$

where $r_{d,\text{fid}} = 147.78$ Mpc and $H_0 = 67.6$ km s⁻¹ Mpc⁻¹.

CONCLUSIONS

(i) The main results of these studies are the independent measured BAO observables $\hat{d}_\alpha(z, z_c)$, $\hat{d}_z(z, z_c)$, and $\hat{d}_\gamma(z, z_c)$ presented in Table III. It is difficult to distinguish the BAO signal from fluctuations of the background. To gain confidence in the results we have repeated the measurements many times with different galaxy selections to obtain different background fluctuations. Requiring successful fits for each of the three independent observables, for each bin of z , allows the use of the consistency relation (8) to discriminate against miss-fits on background fluctuations instead of the BAO signal. The consistency parameter Q also allows quality control of the measurements, see Figure 2. Table III for DR13 data supersedes the corresponding tables in Refs. [8] and [12] for DR12 data.

(ii) From the 18 BAO measurements in Table III, and no other input, we obtain

$$\begin{aligned}\Omega_k &= 0.151 \pm 0.185, \\ \Omega_{DE} + 0.5\Omega_k &= 0.732 \pm 0.052, \\ w_1 &= 0.33 \pm 0.70,\end{aligned}\quad (24)$$

for $\Omega_{DE}(a)$ allowed to vary as in Scenario 4. For $\Omega_k = 0$ and constant $\Omega_{DE}(a)$ we obtain $\Omega_{DE} = 0.716 \pm 0.014$, which may be compared to the independent Planck “TT+lowP+lensing” result (which assumes a Λ CDM cosmology with $\Omega_k = 0$): $\Omega_{DE} = 0.692 \pm 0.012$ [2]. Note that these two results are based on independent cosmological measurements. See Table IV for fits in several scenarios.

TABLE VI: Cosmological parameters obtained from the 18 BAO measurements in Table III plus θ_{MC} from Eq. (9) plus 2 Ly α measurements in Eq. (15) plus A in several scenarios. Corrections for peculiar motions are given by Eq. (11). $N_{eq} = 3.38$. Scenario 1 has $\Omega_{DE}(a)$ constant. Scenario 4 has $\Omega_{DE}(a) = \Omega_{DE}[1 + w_1(1 - a)]$.

A	Scenario 1	Scenario 1	Scenario 4	Scenario 4	Scenario 4	Scenario 4
	1.000 ± 0.021	0.972 ± 0.007	1.000 ± 0.021	1.000 ± 0.021	0.972 ± 0.007	0.972 ± 0.007
Ω_k	0 fixed	0 fixed	0 fixed	-0.006 ± 0.008	0 fixed	-0.009 ± 0.005
$\Omega_{DE} + 2.2\Omega_k$	0.719 ± 0.003	0.719 ± 0.003	0.718 ± 0.004	0.718 ± 0.004	0.715 ± 0.004	0.718 ± 0.004
w_1	n.a.	n.a.	0.05 ± 0.14	0.16 ± 0.20	0.19 ± 0.13	0.24 ± 0.12
$100d_{BAO}$	3.40 ± 0.02	3.39 ± 0.02	3.39 ± 0.03	3.38 ± 0.03	3.36 ± 0.03	3.38 ± 0.03
$\chi^2/\text{d.f.}$	20.3/20	23.8/20	20.1/19	19.6/18	21.1/19	17.8/18

TABLE VII: Final consensus “BAO+FS” measurements of the SDSS DR12 data set [18] (uncertainties are statistical and systematic), and the corresponding BAO parameters $\hat{d}_\alpha(z, z_c)$ and $\hat{d}_z(z, z_c)$ with $z_c = 3.79$. These measurements include the peculiar motion corrections.

z	$D_M r_{d,\text{fid}}/r_d$ [Mpc]	$100\hat{d}_\alpha(z, z_c)$	$H r_d/r_{d,\text{fid}}$ [km s $^{-1}$ Mpc $^{-1}$]	$100\hat{d}_z(z, z_c)$
0.38	$1518 \pm 20 \pm 11$	3.346 ± 0.050	$81.5 \pm 1.7 \pm 0.9$	3.270 ± 0.077
0.51	$1977 \pm 23 \pm 14$	3.332 ± 0.045	$90.5 \pm 1.7 \pm 1.0$	3.375 ± 0.074
0.61	$2283 \pm 28 \pm 16$	3.362 ± 0.047	$97.3 \pm 1.8 \pm 1.1$	3.426 ± 0.074

(iii) From 18 BAO measurements plus θ_{MC} from the CMB we obtain

$$\begin{aligned}\Omega_k &= -0.015 \pm 0.030, \\ \Omega_{DE} + 2.2\Omega_k &= 0.717 \pm 0.004, \\ w_1 &= 0.37 \pm 0.61,\end{aligned}\quad (25)$$

for $\Omega_{DE}(a)$ allowed to vary as in Scenario 4. See Tables V for fits in several scenarios. The cosmological parameters h , $\Omega_b h^2$ and N_{eq} drop out of this analysis. Imposing the constraints $\Omega_k = 0$ and constant $\Omega_{DE}(a)$ obtains $\Omega_{DE} = 0.719 \pm 0.003$.

(iv) Detailed measurements of $\Omega_{DE}(a)$ are presented in Figs. 3 and 4.

(v) From 18 BAO plus θ_{MC} plus 2 Ly α measurements we obtain

$$\begin{aligned}\Omega_k &= -0.013 \pm 0.009, \\ \Omega_{DE} + 2.2\Omega_k &= 0.717 \pm 0.004, \\ w_1 &= 0.34 \pm 0.24, \\ A &= 0.965 \pm 0.014,\end{aligned}\quad (26)$$

when $\Omega_{DE}(a)$ is allowed to vary as in Scenario 4. Note the constraint on A defined in Eq. (19). The corresponding constraint on N_{eq} for $\Omega_b h^2 = 0.0225 \pm 0.0008$, and $h = 0.720 \pm 0.030$ is $N_{eq} = 3.92 \pm 0.40$ corresponding to $N_{\text{eff}} = 4.2 \pm 0.9$ neutrino flavors.

For $\Omega_k = 0$ and constant $\Omega_{DE}(a)$ we obtain $A = 0.9855 \pm 0.0012$. The corresponding constraint on N_{eq} for $\Omega_b h^2 = 0.02226 \pm 0.00023$, and $h = 0.678 \pm 0.009$ is $N_{eq} = 3.20 \pm 0.09$ corresponding to $N_{\text{eff}} = 2.64 \pm 0.20$ neutrino flavors.

(vi) From 18 BAO plus θ_{MC} plus 2 Ly α plus A measurements with $N_{eq} = 3.38$ fixed we obtain the results

shown in Table VI. For $\Omega_{DE}(a)$ allowed to vary as in Scenario 4 and $A = 1.000 \pm 0.021$ we obtain

$$\begin{aligned}\Omega_k &= -0.006 \pm 0.008, \\ \Omega_{DE} + 2.2\Omega_k &= 0.718 \pm 0.004, \\ w_1 &= 0.16 \pm 0.20.\end{aligned}\quad (27)$$

(vii) For all data sets we obtain no tension with the constraints $\Omega_k = 0$ and constant $\Omega_{DE}(a)$.

The SDSS has brought the measurements of $\Omega_{DE}(a)$ with free Ω_k to a new level of precision.

ACKNOWLEDGMENT

Funding for the Sloan Digital Sky Survey IV has been provided by the Alfred P. Sloan Foundation, the U.S. Department of Energy Office of Science, and the Participating Institutions. SDSS-IV acknowledges support and resources from the Center for High-Performance Computing at the University of Utah. The SDSS web site is www.sdss.org.

SDSS-IV is managed by the Astrophysical Research Consortium for the Participating Institutions of the SDSS Collaboration including the Brazilian Participation Group, the Carnegie Institution for Science, Carnegie Mellon University, the Chilean Participation Group, the French Participation Group, Harvard-Smithsonian Center for Astrophysics, Instituto de Astrofísica de Canarias, The Johns Hopkins University, Kavli Institute for the Physics and Mathematics of the Universe (IPMU) / University of Tokyo, Lawrence Berkeley National Laboratory, Leibniz Institut für Astrophysik Potsdam (AIP), Max-Planck-Institut für Astronomie (MPIA

Heidelberg), Max-Planck-Institut für Astrophysik (MPA Garching), Max-Planck-Institut für Extraterrestrische Physik (MPE), National Astronomical Observatories of China, New Mexico State University, New York University, University of Notre Dame, Observatório Nacional / MCTI, The Ohio State University, Pennsylvania State University, Shanghai Astronomical Observatory, United Kingdom Participation Group, Universidad Nacional Autónoma de México, University of Arizona, University of Colorado Boulder, University of Oxford, University of Portsmouth, University of Utah, University of Virginia, University of Washington, University of Wisconsin, Vanderbilt University, and Yale University.

-
- [1] D. J. Eisenstein, H.-J. Seo, and M. White, *ApJ*, 664: 660-674 (2007).
 - [2] C. Patrignani et al. (Particle Data Group), *Chin. Phys. C*, 40, 100001 (2016).
 - [3] Bruce A. Bassett and Renée Hlozek, *arXiv:0910.5224*

- (2009).
- [4] David H. Weinberg et.al., *arXiv:1201.2434* (2013).
- [5] B. Hoeneisen, *arXiv:astro-ph/0009071* (2000).
- [6] Hee-Jong Seo, et al., *ApJ*, 720, 1650 (2010).
- [7] Franco D. Albareti, et al., SDSS Collaboration, *arXiv:1608.02013* (2016).
- [8] B. Hoeneisen, *arXiv:1607.02424* (2016).
- [9] Planck Collab. 2015 Results XIII, *Astron. & Astrophys.* submitted, *arXiv:1502.01589v2*.
- [10] Andreu Font-Ribera et. al., *J. Cosmology Astropart. Phys.* 05, 027 (2014), *arXiv:1311.1767*.
- [11] Timothée Delubac, et al., *arXiv:1404.1801v2* (2014).
- [12] B. Hoeneisen, *arXiv:1608.08486* (2016).
- [13] Shadab Alam, et al. (SDSS-III), *arXiv:1501.00963* (2015).
- [14] John A. Peacock, “Cosmological Physics”, Cambridge University Press (1999).
- [15] M. Chevallier, D. Polarski *Int. J. Mod. Phys. D*10, 213 (2001)
- [16] Eric V. Linder, *Phys.Rev.Lett.* 90:091301 (2003)
- [17] E.M.L. Humphreys et al., *Astrophys. J.*, 775, 13 (2013).
- [18] Shadab Alam et al., *arXiv:1607.03155* (2016).